The Southern Oscillation Revisited: Sea Level Pressures, Surface Temperatures, and Precipitation

KEVIN E. TRENBERTH AND JULIE M. CARON

National Center for Atmospheric Research, Boulder, Colorado*

(Manuscript received 28 January 2000, in final form 15 February 2000)

ABSTRACT

An update is given of the global correlation and regression patterns of sea level pressure associated with the Southern Oscillation, based upon the reanalyses from the National Centers for Environmental Prediction–National Center for Atmospheric Research for 1958–98, a period independent of that of early work. Features over the oceans are better defined than was previously possible and most features prove to be robust, although climate changes such as the 1976 climate shift have evidently altered some important relationships, such as those with Southeast Asia. Associated surface temperature patterns are also shown over the same interval and reveal striking symmetry about the equator. For El Niño, the patterns emphasize the associated broad warming over the tropical central and eastern Pacific, as well as along the west coast of the Americas extending into high latitudes of the Pacific in both hemispheres, and cooling in the central North and South Pacific. Precipitation patterns associated with the Southern Oscillation are given based upon the post-1979 period to include satellite data over the oceans, which emphasizes that the main changes are for a global redistribution of precipitation, so that solely land-based perspectives are biased. While annual mean patterns reveal much of the geographic structure associated with the Southern Oscillation, important seasonal variations are present, especially for sea level pressure and precipitation.

1. Introduction

One of the most prominent sources of interannual variations in weather and climate around the world is the El Niño–Southern Oscillation (ENSO) phenomenon. The existence of a global scale seesaw in surface pressures was first hinted at in the late 1800s, but it was Walker and Bliss (1932, 1937) who documented its characteristics and extent in sea level pressures and associated changes in temperatures and precipitation, and gave it the name Southern Oscillation (SO). Thus the SO is a global-scale teleconnection pattern in the atmosphere and was termed ''southern'' to distinguish it from some other teleconnection patterns (notably the North Pacific and North Atlantic oscillations), which turn out to be of more regional interest.

For many years, interest in the SO lay dormant, perhaps in large part because the role of ENSO in climate variability was diminished from about the 1920s to 1950 or so (Trenberth and Shea 1987). Interest was revived by Troup (1965), who confirmed the robustness of the SO signal, although he noted that the signal was less marked in the recent decades, and especially by Bjerknes (1969), who linked the SO to El Niño and described the role of the Walker circulation and positive feedbacks in ENSO.

Walker and Bliss defined an SO index (SOI) separately for each season, using several variables, and showed patterns of the SO. Troup (1965) retained station pressures as the only element and put the patterns on a more solid footing. But with different definitions of the SOI for each season, there is no continuous measure of the SO variability. Berlage (1957, 1966) used the Djakarta pressures to derive global patterns, often with very short records of data, while Quinn and Burt (1970) used the pressures at Darwin (12.4°S, 130.9°E), in northern Australia. While such SO indices have an advantage of being continuous and homogeneous, they represent only one center of action of the SO and thus include local variations that are not part of the SO. Hence Berlage (1966) and Quinn and Burt (1972) introduced the pressures in the South Pacific Ocean at Easter Island as a part of an SOI, while Pittock (1974) included Tahiti (17.5°S, 149.6°W) values. Trenberth (1976, 1984) showed the need to normalize the values at each center of action *before* taking differences to form an index and further showed that the strongest negative correlations of annual mean pressures anywhere were between Dar-

* The National Center for Atmospheric Research is sponsored by the National Science Foundation.

Corresponding author address: Dr. Kevin E. Trenberth, National Center for Atmospheric Research, P.O. Box 3000, Boulder, CO 80307. E-mail: trenbert@ucar.edu

win and Tahiti at −0.79 (Trenberth 1984), so that this provided the best basis for a simple SOI. That study also showed the need to average in time to obtain at least seasonal (and preferably longer) values, in order to remove nonrepresentative transient and local effects and obtain a measure (i.e., an index) of the actual SO (see also Trenberth and Hoar 1996). The Tahiti minus Darwin SOI is now well established as a standard index, and the results here support its continued use as a representation of the locations of strongest teleconnectivity.

It is now well established that the SO is principally a seesaw (or standing wave) in atmospheric mass involving coherent exchanges of air between the Eastern and Western Hemispheres centered in tropical and subtropical latitudes, with centers of action located over Indonesia and the tropical South Pacific Ocean. The links to higher latitudes are less clear in annual means because of seasonal changes in the teleconnections. The teleconnections tend to be strongest in the winter of each hemisphere and feature alternating sequences of high and low pressures (wave trains) accompanied by distinct standing wave patterns in the jet stream (e.g., Trenberth and Paolino 1981; van Loon and Shea 1987; Trenberth et al. 1998).

Nevertheless, it has taken some time to fully establish the global patterns of the SO. Trenberth (1976) detailed the SO patterns over Australasia and the South Pacific using a combination of station data and regional analyses, and SO patterns became quite well established over the northern extratropics by making use of the gridded hemispheric (poleward of 20°N) sea level pressures, which begin in 1899 (Trenberth and Paolino 1981). Trenberth and Shea (1987) kluged together several of these data sources to provide a revised global map of the SO based upon one point correlations of annual mean sea level or surface pressures with those at Darwin, and this has been widely used and reproduced since.

It is only since the recent reanalyses of the National Centers for Environmental Prediction–National Center for Atmospheric Research (NCEP–NCAR) (Kalnay et al. 1996) that global gridded datasets of sea level pressures exist over a long enough period of time to allow a reexamination of the global SO patterns, and this is the main purpose of this paper. However, for the sake of completeness, we also briefly consider the associated surface temperature and precipitation patterns, although using a much shorter record for the latter. In all cases, we emphasize the need for global information and the perspective that the complete patterns provide.

2. Data

The NCEP–NCAR reanalyses have been extended back in time to 1948. However, the quality declines as the data amounts diminish, and there is considerable evidence that suggests lower quality prior to July 1957, which is when the radiosondes switched from being taken at 0300 and 1500 UTC to the current 0000 and 1200 UTC. Accordingly, we have decided to base the sea level pressure results on the recent 41-yr period from 1958 to 1998. Note that this is an independent period from that of the earlier studies of Walker and Troup, and it includes recent unusual behavior such as the climate jump that occurred around 1976 (Trenberth 1990; Wang 1995; Trenberth and Hoar 1996); this provides an additional challenge to see how well the patterns have stood the test of time.

There was a problem with the NCEP–NCAR reanalyses that affects the quality of the reanalyses over the Southern Hemisphere (SH). The problem arose from the assimilation of PAOBS (see http://wesley.wwb.noaa.gov/paobs/paobs.html), in which the observations were erroneously shifted by 180° in longitude. The error affects 1979–92 (14 yr). PAOBS are produced by the Australians for the data-poor southern oceans and are the product of human analysts who estimate sea level pressure based on satellite data, conventional data, and time continuity. Tests run on the impact of the problem indicate that (i) the SH mid- and high latitudes (40°–60°S) are most affected, (ii) the SH winter months are affected more than the SH summer months, and (iii) the differences decrease rapidly as the timescale increases from synoptic to monthly. Accordingly, the impact on our analysis, which uses seasonal data, is probably fairly small, but it is likely to add some level of noise and thus reduce correlations somewhat over the southern oceans.

The surface temperature dataset is an updated version of the dataset used in the Intergovernmental Panel of Climate Change (IPCC) assessments (e.g., Houghton et al. 1996). The development of this dataset has been well documented (Jones and Briffa 1992; Parker et al. 1994). We compute relationships for the same period as was used for the sea level pressure fields.

Estimates of monthly global patterns of precipitation are only available after 1979 (see Xie and Arkin 1997). We use the Xie–Arkin dataset, called the Climate Prediction Center Merged Analysis of Precipitation. Over land these fields are mainly based on information from rain gauge observations, while over the ocean they are primarily based on satellite estimates made with several different algorithms based on outgoing longwave radiation, and scattering and emission of microwave radiation. Because the latter consist of an integration of spot estimates of precipitation rate, they are subject to considerable sampling uncertainties. Thus the estimates of precipitation utilize several sensors and algorithms and contain considerable uncertainties over the oceans, because there is no basis yet for establishing the truth. In this regard the magnitudes are probably more uncertain than the patterns.

Because ENSO tends to be phase-locked with the annual cycle and preferentially changes sign at about March through May (e.g., Trenberth 1984) we have chosen to define the annual mean to fit the ENSO year of May to April the next year, rather than the calendar year.

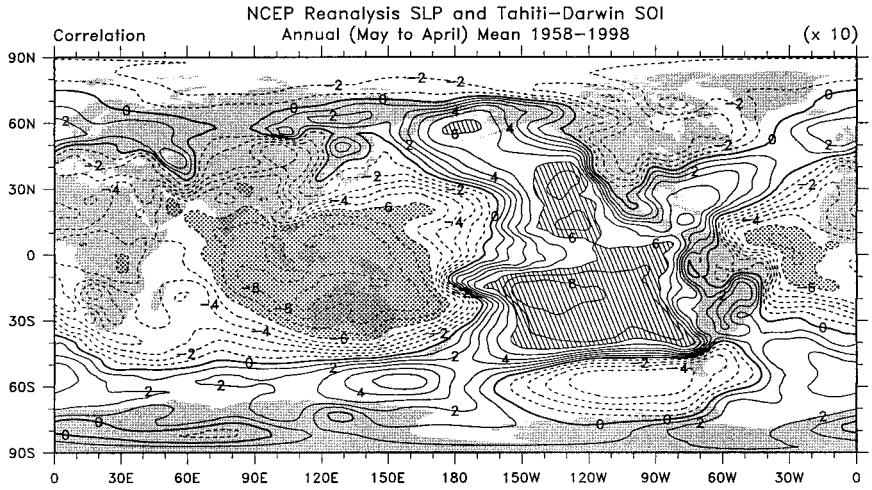

FIG. 1. Correlations of annual mean (May–Apr) of sea level pressure with the SOI for 1958–98. Values >0.6 are hatched and those <-0.6 are stippled.

The long-term monthly means are removed from the data, and only anomalies are used in the regression analysis.

3. Results

a. Sea level pressures

We first computed the correlations with annual mean Darwin pressures as an SOI and found that the Trenberth and Shea (1987) pattern stood up remarkably well. However, it is preferable to use the more complete Tahiti–Darwin SOI to define the patterns. They are quite similar to those using Darwin alone, in every respect except that the correlations are naturally stronger throughout the Pacific, and indeed are marginally stronger in most places around the world, presumably because of the reduction in noise in the SOI.

Figure 1 presents the annual mean pressure correlations with the SOI, while Fig. 2 presents the corresponding regression coefficient and the *t* statistic. The latter indicates statistical significance nearly everywhere (the locations where *t* is greater than 2 in magnitude have corresponding 95% levels of significance), except at very high latitudes in both hemispheres. Values are not significant over much of Eurasia north of 45°N or over the corresponding longitudes over the southern oceans. But significant values are evident over the entire Pacific–North American sector as well as over the southern oceans from Australia to the South Atlantic.

The classical pattern of the SO as a major, mostly wave-one, structure seesaw in the Tropics and subtropics is evident in Fig. 1. However, Fig. 2 regression values, which correspond to those of a normalized SOI of unity (i.e., a one–standard deviation departure), show the much larger pressure departures over the North and South Pacific. Note especially the quadrapole structure over the Australasia–South Pacific region, which has not been well documented previously and which is stronger in absolute terms than the North Pacific link, at least for the annual mean. The latter caveat is important, because the seasonal variability is much greater in the Northern Hemisphere.

Figures 3 and 4 show the corresponding seasonal patterns of the SO for the correlation and regression coefficients. The seasons are the standard ones for March–April–May (MAM), June–July–August (JJA), September–October–November (SON), and December–January–February (DJF). The Indonesian center of action is most extensive in DJF and smallest in area in JJA. This latter season is when the SO potentially influences the Indian monsoon, and this influence seems to have changed with time, as the correlations in that area are weaker than in Troup (1965). This is discussed further by Kumar et al. (1999). DJF is also when the strongest correlations extend into other parts of the Tropics, with values exceeding -0.6 over the western Indian Ocean, Africa, and the Atlantic. Perhaps this is not surprising, given that ENSO is strongest at this time of year (Trenberth 1997). However, the tropical Pacific center of action is weakest in MAM and has the strongest links into the Northern Hemisphere subtropics in JJA and SON. Overall the links are strongest in the SH.

The negative values over the Atlantic extend into the Gulf of Mexico only in JJA and SON, which is the northern hurricane season, and implies higher pressures during El Niño, which can help to suppress Atlantic tropical storm development, as observed. This link also accounts for the connection with rainfall in the Nordeste (of Brazil) (see Figs. 6 and 7, presented later). In the North Atlantic, the strong SO signal in DJF of negative values over the Tropics and positive values (>0.6) near Florida reveals a significant influence to 50°N. In MAM the patterns are even stronger, and a negative region develops over the North Atlantic. Remarkably, this

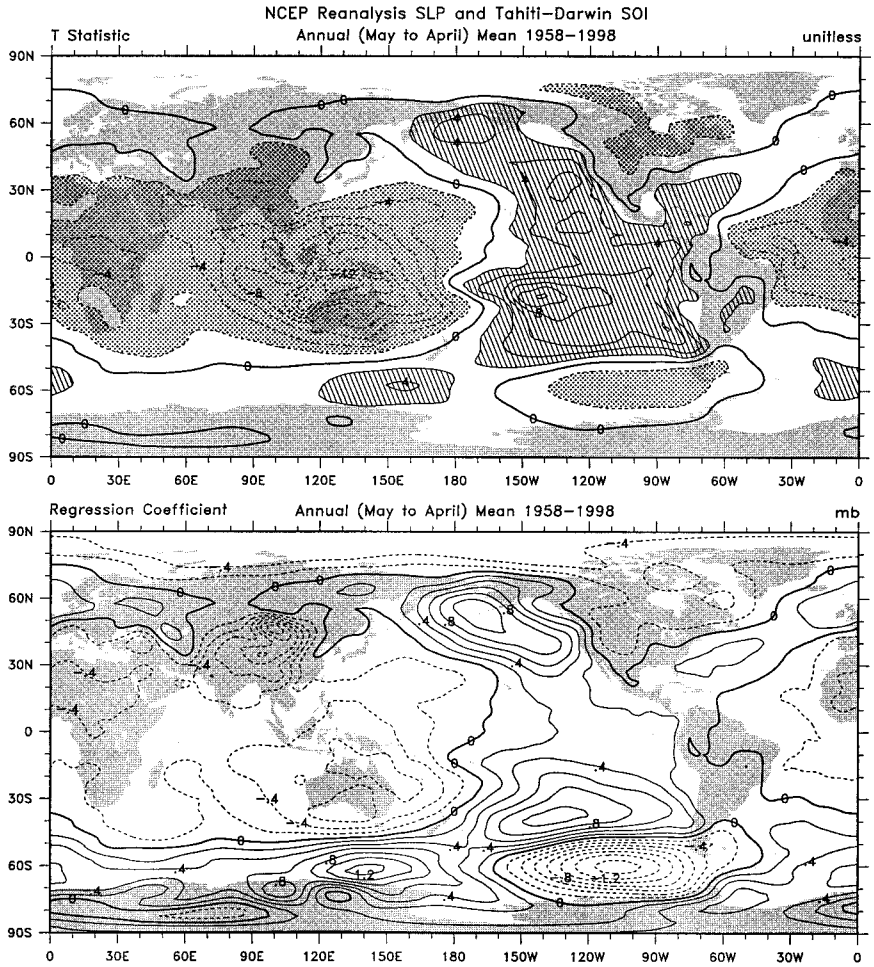

FIG. 2. For the annual mean sea level pressures, shown are the *t* statistic of statistical significance of correlations with the SOI (the contour interval is 2; magnitudes exceeding 2 are significant at the 95% level and are hatched or stippled) and the regression coefficient, in mb, corresponding to a one–standard deviation departure in SOI (the contour interval is 0.2 mb).

structure reverses in JJA, although it is, for the most part, not statistically significant. The seasonal variations over the North Atlantic and Europe are large, but perhaps not surprising if they are indeed teleconnections forced from the Tropics, because small changes in the wavelength and propagation of quasi-stationary Rossby waves become magnified with distance (see Trenberth et al. 1998). Consequently the stability of these patterns, especially in a changing climate, should be suspect.

Highest negative correlations over North America of −0.4 occur in MAM, counter to conventional wisdom, but consistent with the recent droughts and floods in the springs of 1988 and 1993 (Trenberth and Guillemot 1996). The structure of the teleconnection across North America is much more like that of the tropical/Northern Hemisphere pattern than the Pacific–North American teleconnection pattern [see Trenberth et al. (1998) for a review]. The regression coefficient patterns shift the North Pacific center farther to the northwest and more clearly include the Aleutian low center itself in DJF, although the tendency for the Aleutian low to move south and east in El Niño conditions is clear.

The Pacific–South American pattern (Karoly 1989) is clearly evident in the annual mean, but is strongest in SON, and varies in detailed structure. Hence the strong gradient across New Zealand varies from more westerly (in El Niño) in DJF, to southwesterly in MAM and SON, to even southerly in JJA. Note also the nose of the South Pacific center extending toward Chile, with another branch over Uruguay and northern Argentina that is weakest in DJF.

b. Temperature

The surface temperature record unfortunately has a considerable amount of missing data. In particular, at various times large areas are missing over the high latitudes, and parts of Africa and South America. We therefore allow for fairly liberal criteria for computing correlations with few values, although the impact is small.

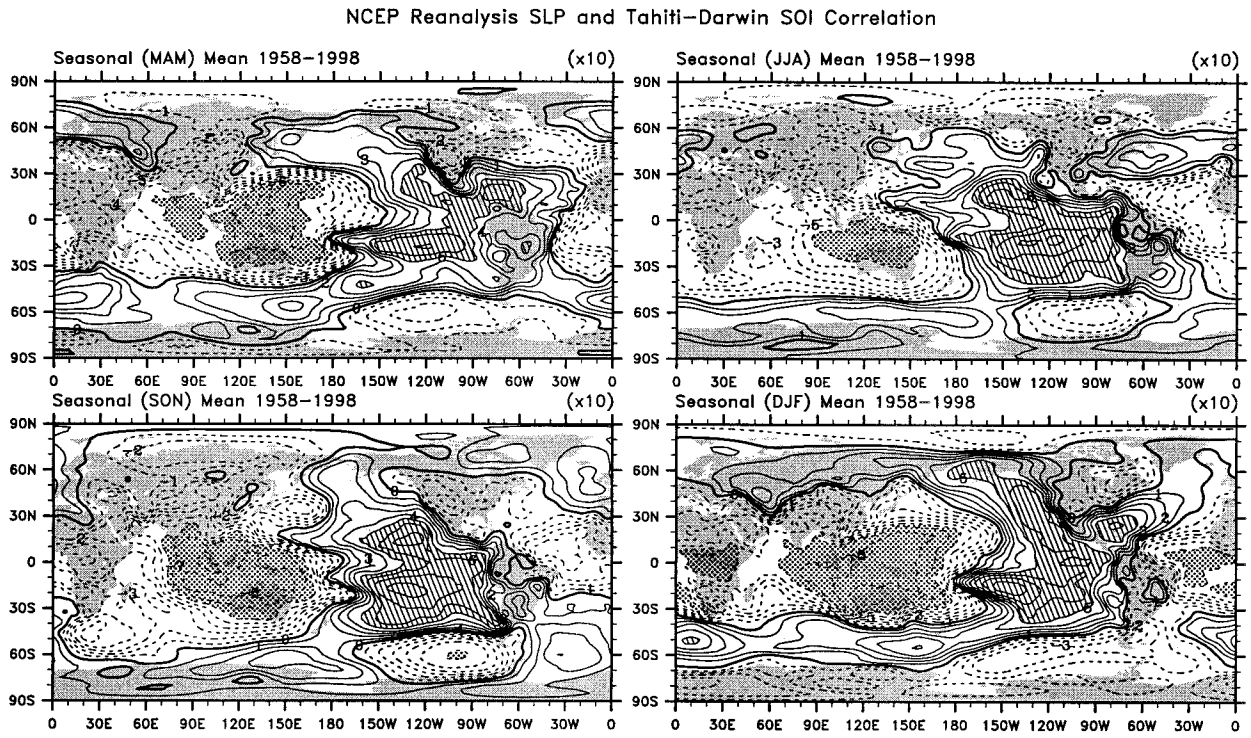

FIG. 3. Correlations of four seasonal means of sea level pressure with the SOI for 1958–98. Values >0.6 are hatched and those <-0.6 are stippled. The contour interval is 0.1.

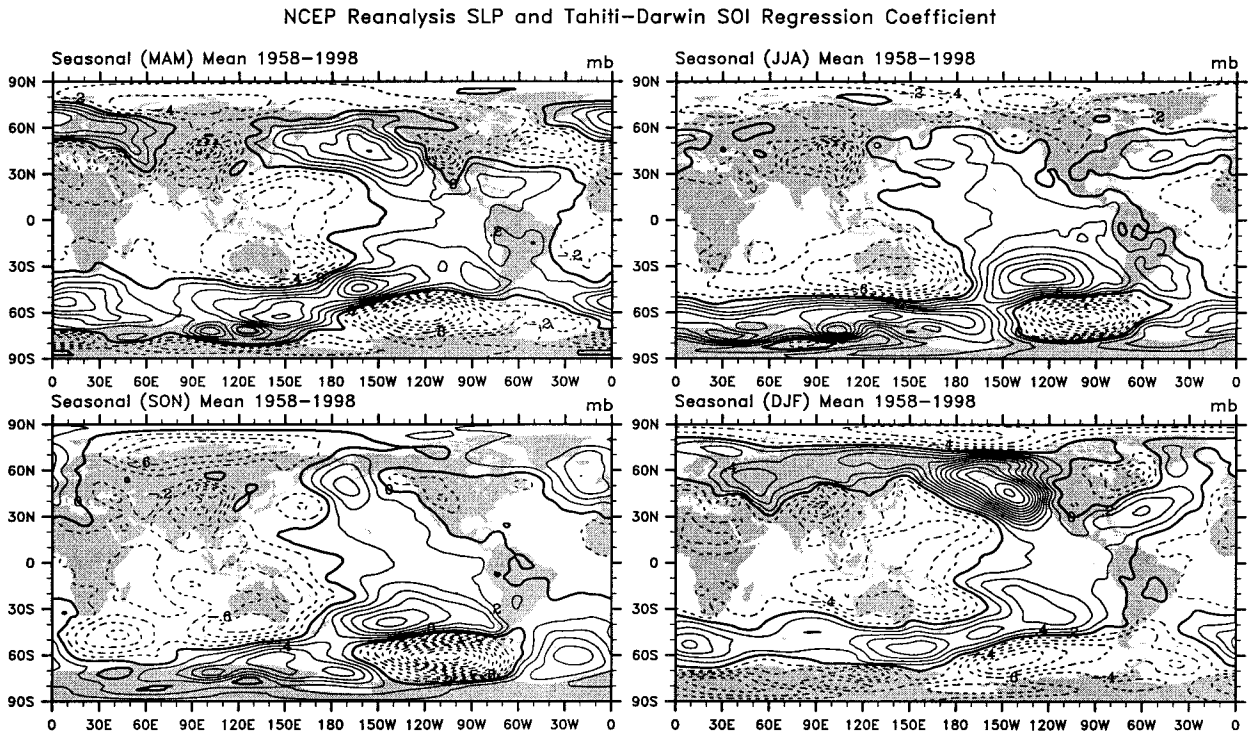

FIG. 4. Regression coefficients with the SOI for seasonal sea level pressure patterns, in mb, corresponding to the correlations in Fig. 3. Negative values are dashed. The contour interval is 0.2 mb.

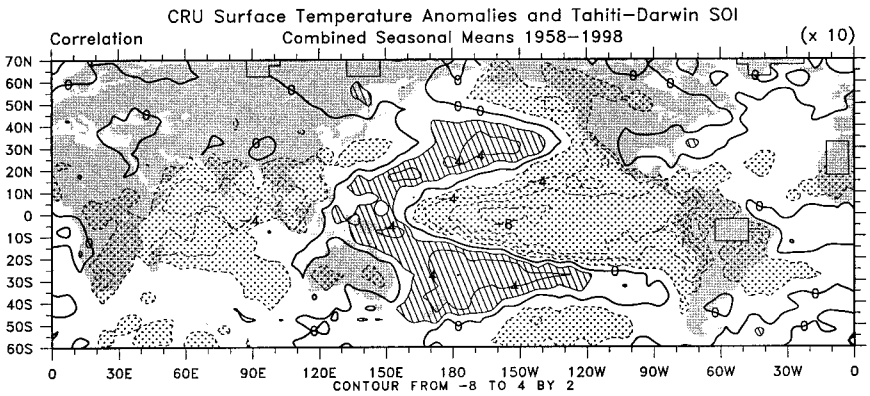

FIG. 5. Correlations of seasonal mean anomalies of surface temperature with the SOI for 1958–98 (164 values). Values >0.2 are hatched and those <−0.2 are stippled. Missing data are blocked out and values are shown for 70°N–60°S.

Examination of the resulting patterns reveals quite similar results in all four seasons except over North America; accordingly, we present only a combined seasonal pattern based on anomalies in all seasons (Fig. 5), in order to ensure that there are adequate data to define the correlations. Consequently, correlations exceeding approximately 0.2 in magnitude are significant and are shaded.

Over North America, the pattern shown in Fig. 5 of positive correlations over the southeastern parts of the United States and negative correlations over the northwestern areas is more distinctive and present in MAM and DJF but not in the summer. Over the oceans, many papers have presented correlations and composites with sea surface temperatures (SSTs) using El Niño–related indices, and these reveal the evolution of the SST patterns and, thus, how the correlation patterns change at various lags, but that aspect is beyond the scope of this paper. Trenberth and Hoar (1996) presented correlations with the SOI and, as in Fig. 5, this showed maximum

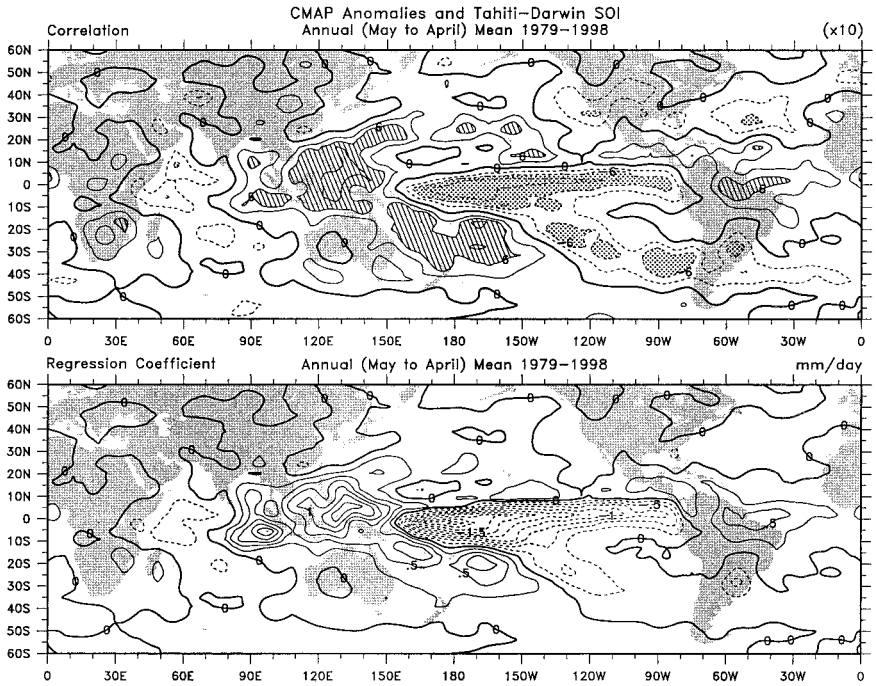

FIG. 6. For annual means (May–Apr) of precipitation amounts, the correlations (top) and regression coefficient in mm day^{-1} (bottom), with the SOI for 1979–98. Values were smoothed to T31 resolution and are cut off at 60°N and 60°S. For the correlations, contours are every 0.2, except that the ±0.2 contour is omitted. Values exceeding 0.4 are significant, and values >+0.6 are hatched and those <−0.6 are stippled. For the regression coefficient, contours are every 0.25 mm day^{-1}.

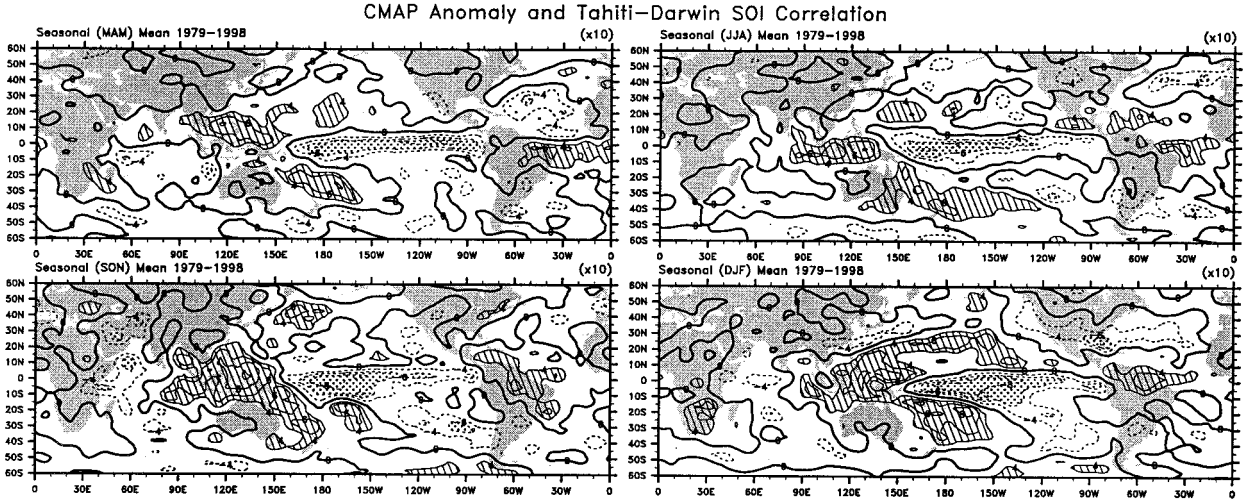

FIG. 7. Correlations of four seasonal means of precipitation with the SOI for 1979–98. Values were smoothed to T31 resolution and contours and shading are as in Fig. 6.

negative correlations (<-0.8) with the so-called Niño-3.4 region (5°N–5°S, 170°–120°W). El Niño is now sometimes thought of as primarily interannual and more confined to the equator, while decadal variability has a broader signature that is stronger and of reverse sign in the extratropical Pacific (e.g., Zhang et al. 1997); however, the relations with the SOI are a combination of both. El Niño warmth extends poleward along the Pacific coast of the Americas in both hemispheres and extends well into western Canada and Alaska. The symmetry about the equator is striking. Correlations in both the North and South Pacific are opposite to those in the central tropical Pacific and also opposite to those farther north (Alaska) and south (50°–65°S, 150°W to South America). El Niño warmth is also present in much of the Indian Ocean and extends over southern Africa as well as parts of South America. Patterns are weak over Asia and the Atlantic north of 30°N.

c. Precipitation

It is important to obtain a global perspective on the rainfall changes rather than the one that has prevailed until now, which uses only station observations (Ropelewski and Halpert 1987, 1989, 1996). For instance the IPCC (Houghton et al. 1996) reported trends in land-based tropical precipitation toward drier conditions, but those trends are dominated by the trends in ENSO and the 1976–77 shift, and the results are highly biased by the island and, thus, station distribution in the Tropics.

Because there are only 20 yr of data for precipitation, the significance level for correlations is 0.41 at the 10% level and 0.49 at the 5% level, so that we have heavily smoothed the results and excluded contours less than 0.4 (other than zero). With few years of data, and because it is well known that anomalies in precipitation depend heavily on the mean field [for instance, large anomalies occur from simple shifts in the location of the intertropical convergence zone (ITCZ) or South Pacific convergence zone (SPCZ)], correlations are not optimal in bringing out relationships, but they are in keeping with the simple approach in this paper. It is desirable to distinguish between positive and negative SO effects, which may not be linear, and one way to examine this facet is to use composite methods. However, there are insufficient data to produce robust global composites at present. Xie and Arkin (1997) presented composites of ''warm minus cold'' events in the tropical Pacific based upon a threshold of 0.5°C for the SST anomalies in the Niño-3 region (5°N–5°S, 150°–90°W). They had only three to six members in each composite with data through 1995.

The patterns found here are quite similar to those of Xie and Arkin (1997) and are not significant at high latitudes. Figure 6 shows the correlations of the SOI with the annual mean precipitation amounts, as well as the corresponding regression coefficient. The latter provide a good idea of the magnitudes in millimeters per day. Figure 7 presents the corresponding seasonal correlations.

The dominant effects are clearly seen throughout the tropical Pacific. In all seasons with El Niño there is an increase in precipitation in the zonal mean in the equatorial region and a net decrease from about 10° to 30° latitude in both hemispheres, but the residuals are small and, overall, below the noise level in the data. Thus the dominant pattern is one of shifts in precipitation, especially the ITCZ and SPCZ, which tend to merge in the central Pacific during El Niño. Patterns are strongest in DJF but are also quite strong in SON, although more confined to the western and central Pacific. Weaker patterns prevail in MAM and especially JJA when the SPCZ is climatologically weaker.

Consistent strong positive correlations of precipita-

tion with the SOI exist over or just off the coast of northeast Brazil, with negative values over southern Brazil and Uruguay. Negative correlations also prevail in the Indian Ocean, except in JJA, and extend over eastern Africa in SON and DJF. Thus, relations with the Asian monsoon for this period are weak to nonexistent (see Kumar et al. 1999). Wet conditions during El Niño are evident across the southern United States in DJF.

While many of the precipitation changes shown here are robust and consistent with the longer historical record, some, such as those over Asia, are particular to this short period. There is a striking resemblance between the precipitation (Fig. 6) and temperature (Fig. 5) patterns, in that warm areas mostly correspond to wet areas. This suggests that local evaporation is an important influence in addition to the changes in atmospheric circulation (Fig. 1). An important point to emphasize here is that the precipitation changes are present throughout the global Tropics, and the historical picture from just land-based stations is quite distorted.

4. Concluding remarks

The primary purpose of this paper has been to update the patterns of sea level pressure associated with the Southern Oscillation. The associated temperature and precipitation fields are also presented and discussed in section 3. Although the annual mean patterns define much of the SOI spatial structures, some important seasonal variants exist, more so in the sea level pressure and implied atmospheric circulation, and in precipitation, than in surface temperature. The period used is independent of that when the SO was initially defined and mapped, and most of the features are remarkably robust. Evidently, some facets are slowly changing as the climate changes. The figures presented here are available online at http://www.cgd.ucar.edu/cas/papers/jclim2000/soi.html.

Acknowledgments. This research was sponsored by the NOAA Office of Global Programs under Grant NA56GP0247 and by joint NOAA/NASA Grant NA87GP0105.

REFERENCES

Berlage, H. P., 1957: Fluctuations of the general atmospheric circulation of more than one year, their nature and prognostic value. *Roy. Neth. Meteor. Inst. Meded. Verh.,* **69,** 152 pp.

——, 1966: The Southern Oscillation and world weather. *Roy. Neth. Meteor. Inst. Meded. Verh.,* **88,** 152 pp.

Bjerknes, J., 1969: Atmospheric teleconnections from the tropical Pacific. *Mon. Wea. Rev.,* **97,** 103–172.

Houghton, J. T., F. G. Meira Filho, B. A. Callander, N. Harris, A. Kattenberg, and K. Mask, Eds., 1996: *Climate Change 1995: The Science of Climate Change.* Cambridge University Press, 572 pp.

Jones, P. D., and K. R. Briffa, 1992: Global surface air temperature variations over the twentieth century. Part 1: Spatial, temporal and seasonal details. *Holocene,* **2,** 174–188.

Kalnay, E., and Coauthors, 1996: The NCEP/NCAR 40-Year Reanalysis Project. *Bull. Amer. Meteor. Soc.,* **77,** 437–471.

Karoly, D. J., 1989: Southern Hemisphere circulation features associated with El Niño–Southern Oscillation events. *J. Climate,* **2,** 1239–1252.

Kumar, K. K., B. Rajagopalan, and M. A. Cane, 1999: On the weakening relationship between the Indian monsoon and ENSO. *Science,* **284,** 2156–2159.

Parker, D. E., P. D. Jones, C. K. Folland, and A. Bevan, 1994: Interdecadal changes of surface temperatures since the late 19th century. *J. Geophys. Res.,* **99,** 14 373–14 399.

Pittock, A. B., 1974: Global interactions in stratosphere and troposphere. *Proc. Conf. on Structure, Composition and General Circulation of the Upper and Lower Atmosphere and Possible Anthropogenic Perturbations,* Vol. II, Melbourne, Australia, IAMAP, 716–726.

Quinn, W. H., and W. V. Burt, 1970: Prediction of abnormally heavy precipitation over the equatorial Pacific dry zone. *J. Appl. Meteor.,* **9,** 20–28.

——, and ——, 1972: Use of the Southern Oscillation in weather prediction. *J. Appl. Meteor.,* **11,** 616–628.

Ropelewski, C. F., and M. S. Halpert, 1987: Global and regional scale precipitation patterns associated with the El Niño/Southern Oscillation. *Mon. Wea. Rev.,* **115,** 1606–1626.

——, and ——, 1989: Precipitation patterns associated with the high index phase of the Southern Oscillation. *J. Climate,* **2,** 268–284.

——, and ——, 1996: Quantifying Southern Oscillation–precipitation relationships. *J. Climate,* **9,** 1043–1059.

Trenberth, K. E., 1976: Spatial and temporal variations of the Southern Oscillation. *Quart. J. Roy. Meteor. Soc.,* **102,** 639–653.

——, 1984: Signal versus noise in the Southern Oscillation. *Mon. Wea. Rev.,* **112,** 326–332.

——, 1990: Recent observed interdecadal climate changes in the Northern Hemisphere. *Bull. Amer. Meteor. Soc.,* **71,** 988–993.

——, 1997: The definition of El Niño. *Bull. Amer. Meteor. Soc.,* **78,** 2771–2777.

——, and D. A. Paolino, 1981: Characteristic patterns of variability of sea level pressure in the Northern Hemisphere. *Mon. Wea. Rev.,* **109,** 1169–1189.

——, and D. J. Shea, 1987: On the evolution of the Southern Oscillation. *Mon. Wea. Rev.,* **115,** 3078–3096.

——, and C. J. Guillemot, 1996: Physical processes involved in the 1988 drought and 1993 floods in North America. *J. Climate,* **9,** 1288–1298.

——, and T. J. Hoar, 1996: The 1990–1995 El Niño–Southern Oscillation Event: Longest on record. *Geophys. Res. Lett.,* **23,** 57–60.

——, G. W. Branstator, D. Karoly, A. Kumar, N.-C. Lau, and C. Ropelewski, 1998: Progress during TOGA in understanding and modeling global teleconnections associated with tropical sea surface temperatures. *J. Geophys. Res.,* **103,** 14 291–14 324.

Troup, A. J., 1965: The Southern Oscillation. *Quart. J. Roy. Meteor. Soc.,* **91,** 490–506.

van Loon, H., and D. J. Shea, 1987: The Southern Oscillation. Part VI: Anomalies of sea level pressure on the Southern Hemisphere and of Pacific sea surface temperature during the development of a warm event. *Mon. Wea. Rev.,* **115,** 370–379.

Walker, G. T., and E. W. Bliss, 1932: World Weather V. *Mem. Roy. Meteor. Soc.,* **4** (36), 53–84.

——, and ——, 1937: World Weather VI. *Mem. Roy. Meteor. Soc.,* **4** (39), 119–139.

Wang, B., 1995: Interdecadal changes in El Niño onset in the last four decades. *J. Climate,* **8,** 267–285.

Xie, P., and P. A. Arkin, 1997: Global precipitation: A 17-year monthly analysis based on gauge observations, satellite estimates, and numerical model outputs. *Bull. Amer. Meteor. Soc.,* **78,** 2539–2558.

Zhang, Y., J. M. Wallace, and D. S. Battisti, 1997: ENSO-like interdecadal variability: 1900–93. *J. Climate,* **10,** 1004–1020.